



## Nearly five-year continuous atmospheric measurements of black carbon over a suburban area in central France

El. Mehdi El. Baramoussi, Yangang Ren, Chaoyang Xue, Ibrahim Ouchen, Véronique Daële, Patrick Mercier, Christophe Chalumeau, Frédéric L.E. Fur, Patrice Colin, Abderrazak Yahyaoui, et al.

### ► To cite this version:

El. Mehdi El. Baramoussi, Yangang Ren, Chaoyang Xue, Ibrahim Ouchen, Véronique Daële, et al.. Nearly five-year continuous atmospheric measurements of black carbon over a suburban area in central France. *Science of the Total Environment*, 2022, 858, pp.159905. 10.1016/j.scitotenv.2022.159905 . hal-03880412

**HAL Id: hal-03880412**

**<https://hal.science/hal-03880412>**

Submitted on 13 Dec 2022

**HAL** is a multi-disciplinary open access archive for the deposit and dissemination of scientific research documents, whether they are published or not. The documents may come from teaching and research institutions in France or abroad, or from public or private research centers.

L'archive ouverte pluridisciplinaire **HAL**, est destinée au dépôt et à la diffusion de documents scientifiques de niveau recherche, publiés ou non, émanant des établissements d'enseignement et de recherche français ou étrangers, des laboratoires publics ou privés.

# Nearly Five-Year Continuous Atmospheric Measurements of Black Carbon over a Suburban Area in Central France

EI Mehdi EI Baramoussi<sup>1, 2, ‡</sup>, Yangang Ren<sup>2, 3, ‡ \*</sup>, Chaoyang Xue<sup>4</sup>, Ibrahim Ouchen<sup>1</sup>,  
Véronique Daële<sup>2</sup>, Patrick Mercier<sup>5</sup>, Christophe Chalumeau<sup>5</sup>, Frédéric LE Fur<sup>5</sup>,  
Patrice Colin<sup>5</sup>, Abderrazak Yahyaoui<sup>5</sup>, Oliver Favez<sup>6</sup>, Abdelwahid Mellouki<sup>2, 7 \*</sup>

<sup>1</sup> Earth Sciences Department, Scientific Institute, Mohammed V University, Rabat  
10106, Morocco

<sup>2</sup> Institut de Combustion Aérothermique, Réactivité et Environnement, Centre  
National de la Recherche Scientifique (ICARE-CNRS), Observatoire des Sciences de  
l'Univers en région Centre (OSUC), CS 50060, 45071 Orléans cedex02, France

<sup>3</sup> Research Center for Eco-Environmental Sciences, Chinese Academy of Sciences,  
Beijing, 100085, PR China

<sup>4</sup> Laboratoire de Physique et Chimie de l'Environnement et de l'Espace (LPC2E),  
CNRS – Université Orléans – CNES (UMR 7328), 45071 Orléans Cedex 2, France

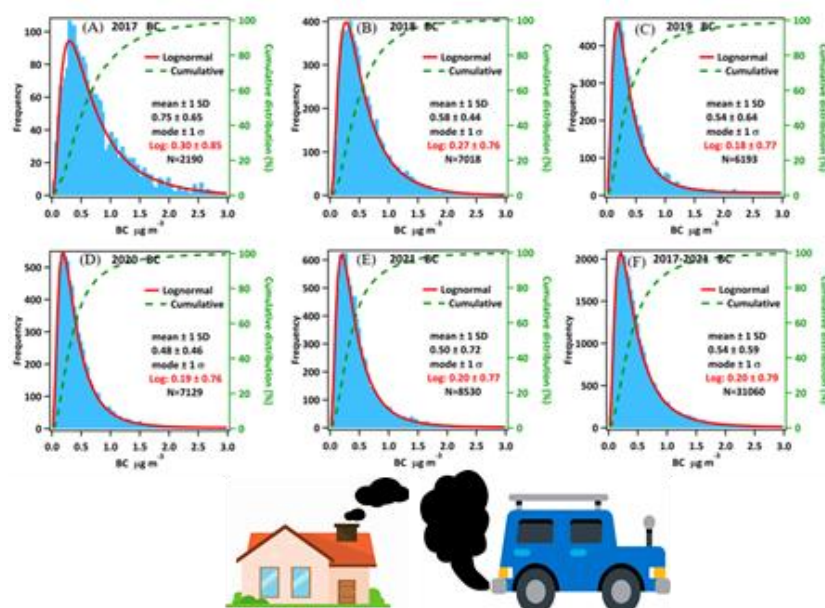
<sup>5</sup> Lig'Air- Association de surveillance de la qualité de l'air en région Centre-Val de  
Loire, 45590 Saint-Cyr-en-Val, France

<sup>6</sup> Institut National de l'Environnement Industriel et des Risques, Parc Technologique  
ALATA, Verneuil-en-Halatte, France

<sup>7</sup> Environment Research Institute, School of Environmental Science and Engineering,  
Shandong University, Qingdao 266237, China

‡ These authors contributed equally to this work

Correspondence \*: Yangang Ren ([ygren@rcees.ac.cn](mailto:ygren@rcees.ac.cn)); Abdelwahid Mellouki  
([mellouki@cnrs-orleans.fr](mailto:mellouki@cnrs-orleans.fr)) Institute for Aerothermic Combustion Reactivity and  
Environment



## Highlights:

1. Five-year BC measurements were conducted in a suburban area in central France.
2. Strong seasonal variations and weekend effects were observed.
3. Biomass burning contributed to more than half of winter BC.
4. Lockdown in cold season and warm season had reverse effect on BC concentration.

## Abstract:

Atmospheric black carbon (BC) concentration over a nearly 5 year period (mid-2017 - 2021) was continuously monitored over a suburban area of Orléans city (France). Annual mean atmospheric BC concentration were  $0.75 \pm 0.65$ ,  $0.58 \pm 0.44$ ,  $0.54 \pm 0.64$ ,  $0.48 \pm 0.46$  and  $0.50 \pm 0.72 \mu\text{g m}^{-3}$ , respectively, for the year of 2017, 2018, 2019, 2020 and 2021. Seasonal pattern was also observed with maximum concentration ( $0.70 \pm 0.18 \mu\text{g m}^{-3}$ ) in winter and minimum concentration ( $0.38 \pm 0.04 \mu\text{g m}^{-3}$ ) in summer. We found a different diurnal pattern between cold (winter and fall) and warm (spring and summer) seasons. Further, fossil fuel burning contributed more

than 90% of atmospheric BC in the summer and biomass burning had a contribution equivalent to that of the fossil fuel in the winter. Significant week days effect on BC concentrations was observed, indicating the important role of local emissions such as car exhaust in BC level at this site. The behavior of atmospheric BC level with COVID-19 lockdown was also analyzed. We found that during the lockdown in warm season (first lockdown: 27 March - 10 May 2020 and third lockdown 17 March - 3 May 2021) BC concentration were lower than in cold season (second lockdown: 29 October–15 December 2020), which could be mainly related to the BC emission from biomass burning for heating. This study provides a long-term BC measurement database input for air quality and climate models. The analysis of especially weekend and lockdown effect showed implications on future policymaking toward improving local and regional air quality as well.

**Keyword:**

Black carbon, measurements, long-term, seasonal pattern, weekend effect, lockdown.

## 1. Introduction

Black carbon (BC) is a primary aerosol emitted directly from incomplete combustion processes such as vehicle exhausts (especially unfiltered diesel type), domestic and industrial coal, heavy oil and wood burning, as well as forest and vegetation fires (WHO, 2012). As a component of atmospheric particulate matter (PM), BC plays an important role in the aerosol-planetary boundary layer (PBL) interactions that can for example enhance the haze pollution (Ding et al., 2016; Zhang et al., 2020).

BC is recognized as an efficient proxy of negative impacts on human health by causing morbidity and premature mortality (Silva et al., 2013). Because of their small diameter ( $\leq 2.5 \mu\text{m}$ , PM<sub>2.5</sub>), BC particles can enter deep into the lungs and the bloodstream to cause cardiovascular and respiratory diseases which may lead to premature death (Anenberg et al., 2011; Gong et al., 2019; Li et al., 2016; Y. Wang et al., 2021). In addition, BC affects visibility and harms ecosystems. BC aerosols play an important role in the climate system, they strongly absorb solar radiation and warm the atmosphere. BC is the second climate forcing agent after CO<sub>2</sub> with a positive radiative forcing of  $1.1 \text{ W m}^{-2}$  (Pörtner et al., 2022). Because of its short atmospheric lifetime, estimated to be of a few days to a few weeks, it has been suggested that mitigation of its emissions is one of the most effective strategies for slowing climate change. The climate will respond quickly to reductions of black carbon, especially in remote regions like the arctic where the warming and melting of snow and ice could be slowed (AMAP, 2015; Sand et al., 2016; WMO, 2016).

Because of its impact on global warming, human health and ecosystems, a large body of research and monitoring activities have been dedicated to the understanding of the atmospheric behavior of BC (Cui et al., 2021; Garrido et al., 2014; Kutzner et al., 2018; Singh et al., 2018) and to take actions to reduce its emissions since it could be considered as a key pollutant to abate from anthropogenic sources.

In the present paper, we report hourly, monthly, and yearly average concentrations and near five years trend of BC levels from September 2017 to December 2021 at the Voltaire supersite at the CNRS Campus (Orléans, France) to trace the major outflow pathways and transport mechanisms for the area of the interest in the present work.

## 2. Methodology

### 2.1. Measurement Site

Real-time continuous measurements of BC were made at the Super-Site Voltaire located in the campus of the National Scientific Research Centre (CNRS) in Orléans, France, as shown in Figure 1, about 8 km south of the Orléans city center ( $47^{\circ}50'16.80''\text{N}$ ,  $1^{\circ}56'39.34''\text{E}$ ). The site is mostly surrounded by grass and trees with no obstructing buildings around it within 50 m. In addition to BC, the site is also equipped with instruments to measure  $\text{O}_3$  and  $\text{NO}_x$ .

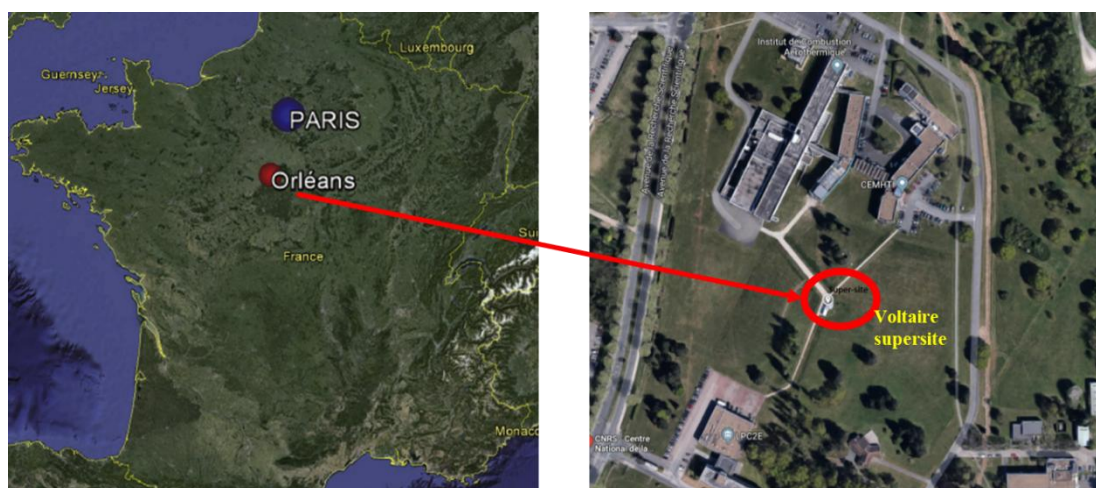


**Figure 1.** Screenshot of the Voltaire sampling site at the CNRS campus (Orléans-France,  $47^{\circ}50'16.80''\text{N}$ ,  $1^{\circ}56'39.34''\text{E}$ ).

### 2.2. Instrumentation

An aethalometer model AE33-7 (Magee Scientific Inc.) with a  $\text{PM}_{2.5}$  inlet was used to measure aerosol BC in real time from September 2017 to December 2021. The AE33 collects particles continuously by flowing air stream through a filter tape. Air is pumped through an inlet at the desired flow rate of 5.0 L/min. The aerosol analysis,

done at seven optical wavelengths (370, 470, 520, 590, 660, 880, 950 nm), is made by measuring the transmission of light through one portion of the filter tape containing the sample, versus the transmission through an unloaded portion of the filter tape which acts as reference. The instrument calculates the instantaneous concentration of optically-absorbing particles from the change of the attenuation of light transmitted through the particle-laden filter. Two measurements are made simultaneously from two sample spots with different rates of accumulation of the sample and the results are combined mathematically to eliminate nonlinearities and provide the compensated particle light absorption and BC mass concentration.

The AE33 calculates BC concentrations with high temporal resolution by analyzing the attenuation of light transmission over time. The BC measurement is extracted from the absorption coefficient measurement at 880 nm. The other wavelengths can be used to estimate the contributions of different combustion sources. The optical attenuation (*ATN*) is calculated from the measurement of the light intensity measured through the “clean” filter band ( $I_0$ ) and measured through the particle-laden band ( $I$ ) using the following mathematical law:

$$ATN = -100 \ln(I/I_0)$$

The particle attenuation coefficient ( $b_{atn}$ ) is calculated by taking into account the area of the measurement ( $S$ ), the flow rate ( $F_{in}$ ) and the sampling time ( $\Delta t$ ) between two *ATN* measurements. Thus the attenuation coefficient,  $b_{atn}$ , induced by the particles deposited, expressed in  $m^{-1}$ , is given by:

$$b_{atn} = S \times (\Delta ATN/100)/(F_{in} \times \Delta t)$$

The flow rate  $F_{in}$  is corrected by a leakage factor,  $\xi$ , which represents the loss of flow in the optical chamber. It constitutes the difference between the flow measured at the input of the instrument and the actual flow rate passing through the filter:

$$F_{in} = F_{out} \times (1 - \xi)$$

$F_{out}$  being the measured flow rate and  $F_{in}$  the actual flow through the band.

On the other hand, the attenuation coefficient  $b_{atn}$  is corrected for the amount of light scattered by the filter strip. Thus, the absorption coefficient of the particles,  $b_{abs}$ , represents the amount of light absorbed by the particles:

$$b_{abs} = b_{atn}/C$$

C is the diffusion coefficient of the filter strip. Hence BC concentration will be obtained from :

$$BC = b_{abs}/\sigma_{air}$$

$\sigma_{air}$  is the mass absorption cross-section, within loading effect compensation,

$$BC = BC_{measured}/(1 - k*ATN)$$

k is the compensation parameter, and the final equation:

$$BC = \frac{S \times (\Delta ATN/100)}{F_1 \times (1 - \xi) * \sigma_{air} \times C \times (1 - k \times ATN_1) \times \Delta t}$$

BC emissions could be apportioned to the source of biomass burning ( $BC_{bb}$ ) and fossil fuel ( $BC_{ff}$ ) based on the Sandradewi et al. (2008) model. This model is based on the difference in absorption coefficient wavelength dependencies, with optical absorption coefficient being a sum of biomass burning and fossil fuel burning fractions. Hence  $BC_{bb}$  and  $BC_{ff}$  are calculated as:

$$BC_{bb} = BB * BC$$

$$BC_{ff} = BC * (1 - BB)$$

With BB (%) is the portion of biomass burning related to total BC, and calculated using a series of equations:

$$b_{abs}(470 \text{ nm})_{ff} / b_{abs}(470 \text{ nm})_{ff} = (470/950)^{-aff}$$

$$b_{abs}(470 \text{ nm})_{bb} / b_{abs}(470 \text{ nm})_{bb} = (470/950)^{-abb}$$

$$b_{abs}(470 \text{ nm}) = b_{abs}(470 \text{ nm})_{ff} + b_{abs}(470 \text{ nm})_{bb}$$

$$b_{abs}(950 \text{ nm}) = b_{abs}(950 \text{ nm})_{ff} + b_{abs}(950 \text{ nm})_{bb}$$

$$BB(\%) = \frac{b_{abs}(950 \text{ nm})_{bb}}{b_{abs}(950 \text{ nm})}$$



where  $b_{\text{abs}}(\lambda)$  is absorption coefficient,  $\lambda$  is wavelength,  $b_{\text{abs}}(\lambda)_{\text{ff}}$  a fossil fuel fraction and  $b_{\text{abs}}(\lambda)_{\text{bb}}$  a biomass burning fraction of absorption coefficient. Ångström exponents:  $\alpha_{\text{ff}}=1$  for fossil fuel and  $\alpha_{\text{bb}}=2$  for biomass.

### 3. Results and Discussion

#### 3.1. Data Overview and Comparisons with Other Sites

The measurements of BC were made from mid-September 2017 up to end December 2021. Technical issues and maintenance of the instruments led to the loss of some data for the period covering January 2018 – December 2021. For this specific period, more than 71% of data has been recorded (Figure S1). Figure 2 shows an overview of measured BC in the present work. In general, the measurement period was characterised by a fairly good air quality in the area of interest to our study, without heavy pollution days. BC was generally lower than  $2 \mu\text{g m}^{-3}$  with few exceptions reaching  $4 \mu\text{g m}^{-3}$ . The annual mean atmospheric BC concentration was  $0.75 \pm 0.65$ ,  $0.58 \pm 0.44$ ,  $0.54 \pm 0.64$ ,  $0.48 \pm 0.46$  and  $0.50 \pm 0.72 \mu\text{g m}^{-3}$ , respectively, for the years 2017, 2018, 2019, 2020 and 2021 as shown in Figure 3. The annual mean of BC concentrations measured in suburban Orléans city, were 3 to 30 times lower than reported in other larger European and non-European cities as displayed in Table 1. Note that Orléans is a medium size city, with not much industry and traffic and a population of about 120000 inhabitants.

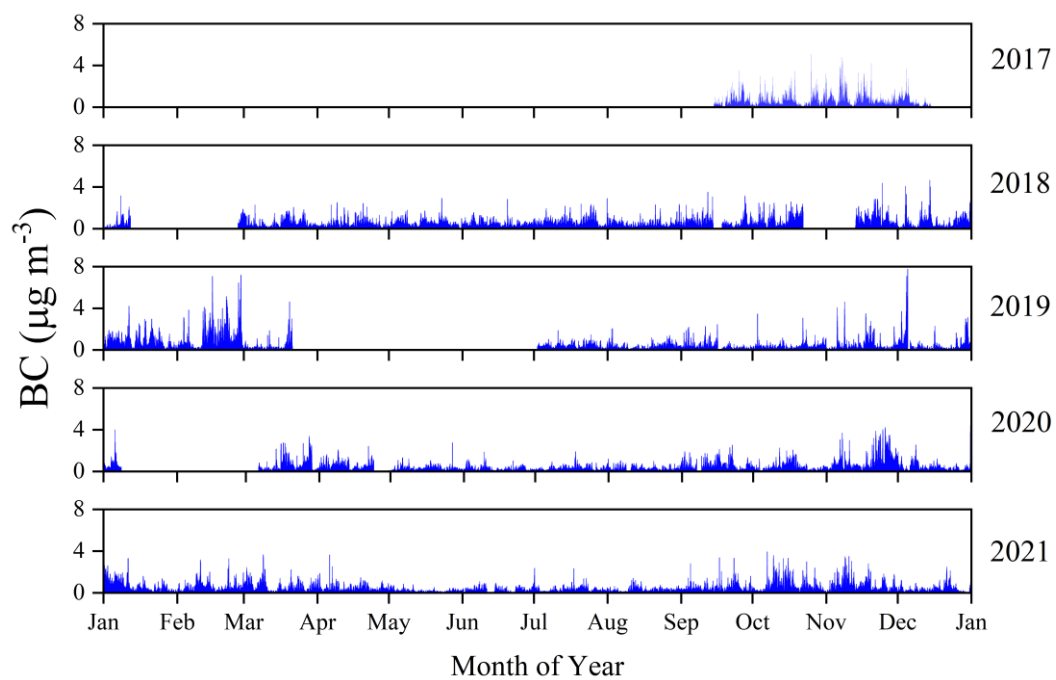


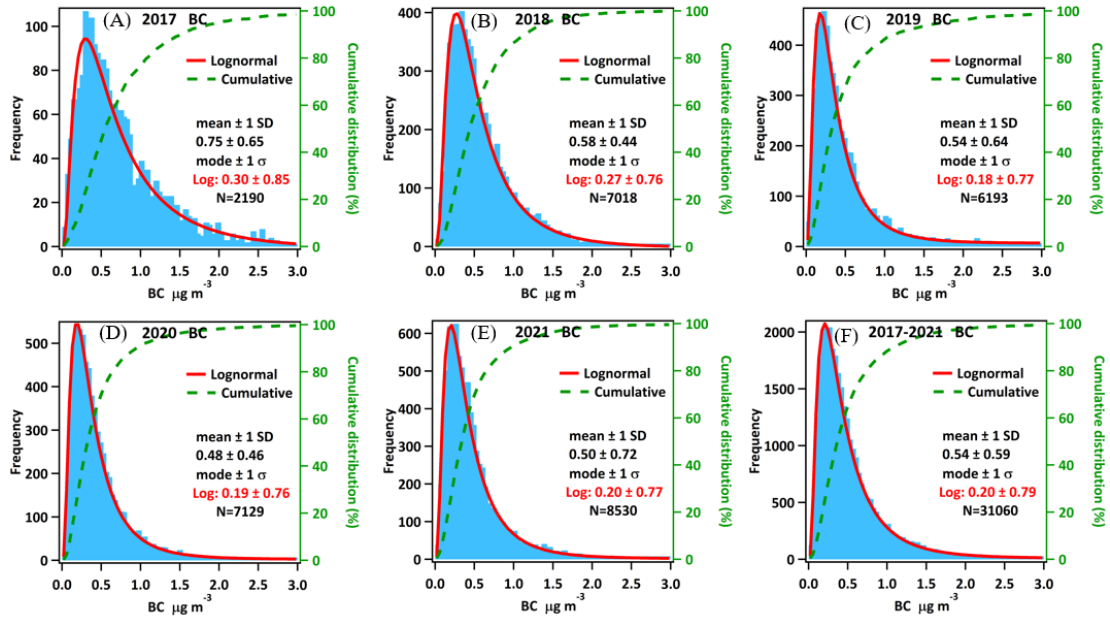
**Figure 2.** BC measurements during 2017-2021 in Orléans city.

**Table 1.** BC measurement in this work and compared with literatures.

City	Study year	BC $\pm$ SD ( $\mu\text{g m}^{-3}$ )	Reference
Barranquilla, Colombia	2018	$16.1 \pm 16.54$	Blanco-Donado et al., (2022)
São Paulo, Brazil	2017	$8.5 \pm 8.4$ Weekday $5.2 \pm 13.9$ Weekday	Krecl et al., (2018)
Macau, China	2016	$4.0 \pm 2.6$ (morning) $3.1 \pm 1.9$ (afternoon)	B. Liu et al., (2019)
Shanghai, China	2016	$10.8 \pm 3.5$	M. Liu et al., (2019)
Shanghai, China	2015	$11.8 \pm 9.8$	Lei et al., (2017)
Brisbane, Australia	2015	$4.4 \pm 7.3$	Williams and Knibbs, (2016)
Londrina, Brazil	2015	$6.35 \pm 20.0$ (morning) $5.10 \pm 14.7$ (afternoon)	Targino et al., (2016)
Shanghai, China	2014	$7.28 \pm 1.63$ $9.43 \pm 1.70$ $8.62 \pm 2.57$	Li et al., (2015)
Bogota, Colombia	2013	$25.6 \pm 39.2$	Franco et al., (2016)
Minneapolis, USA	2012	$2.5 \pm 1.4$ (morning) $0.7 \pm 1.6$ (afternoon)	Hankey and Marshall, (2015)
Stockholm, Sweden	2011	$2.4 \pm 3.6$	Krecl et al., (2014)
Berkeley, USA	2011	$1.76 \pm 2.58$ low traffic $2.06 \pm 3.23$ high traffic	Jarjour et al., (2013)
Helsinki, Finland	2011	$7.8 \pm 4.3$	Okokon et al., (2017)
Rotterdam, Finland	2011	$6.4 \pm 3.3$	
Thessaloniki, Finland	2011	$10.9 \pm 9.9$	
Barcelona, Spain	2009	16.7	de Nazelle et al., (2012)
Orléans, France	2017	$0.75 \pm 0.65$	This work
Orléans, France	2018	$0.58 \pm 0.44$	This work
Orléans, France	2019	$0.54 \pm 0.64$	This work

City	Study year	BC $\pm$ SD ( $\mu\text{g m}^{-3}$ )	Reference
Orléans, France	2020	$0.48 \pm 0.46$	This work
Orléans, France	2021	$0.50 \pm 0.72$	This work

189



190

191

**Figure 1.** Histograms of BC measurement data from 2017 to 2021.

192

### 193 3.2. Nearly 5 years trend of BC in Orléans

194 The continuous observations over a period of nearly 5 years (mid 2017 – end  
195 2021) in Orléans (central France) provides data to check to tendency of the  
196 atmospheric BC concentration in the region for the last five years. Since only 25% of  
197 BC data was obtained in 2017 (Figure S1), we only used data from 2018 to 2021 to  
198 discuss the trend observed in this work. As shown in Figure 4, a decrease of 3.6% per  
199 year is observed in the studied area. It has to be noted that a general decrease in the  
200 atmospheric BC has been reported in many other areas over Europe resulting mainly  
201 from the mitigation policies of air pollution in Europe since 1990's. For example, a  
202 decrease as high as  $8 \pm 3$  % per year has been reported by Singh et al. (2018) at  
203 Marylebone road in London. Sun et al. (2020) reported a decreasing trend of BC  
204 concentration between -13.1 and -1.7 % per year from 2009 to 2018 over Germany.

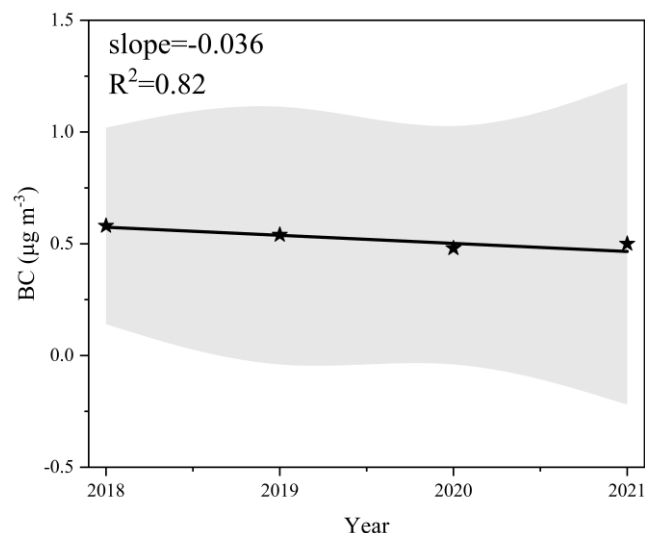


**Figure 2.** Four yeras trend of BC at the Voltaire supersite during the period 2018-2021.

### 3.2. Seasonal variations

The diurnal profile of BC under different seasons at the site for the entire measurement period is depicted in Figure 5. This figure shows that the highest BC concentration occurred in winter, followed by autumn, spring and summer, with seasonal mean ( $\pm$ SD) values of  $0.70 \pm 0.18$ ,  $0.64 \pm 0.11$ ,  $0.48 \pm 0.11$  and  $0.38 \pm 0.04$   $\mu\text{g m}^{-3}$ , respectively. Compared to spring and summer, the elevated BC concentrations in winter and autumn were likely related to the common occurrence of wood burning for household heating and relative lower boundary height due to cold weather, as reported by other studies (Fuller et al., 2014; Genberg et al., 2013).

Figure 5 indicates also that the diurnal variations of BC in winter and autumn were similar, within one significant morning peak during the morning rush hours and second significant peak in the evening. In spring and summer, BC concentration also increased in the morning and peaked during the morning rushing hours. However, the morning peak shifted from 7:00 (Local time, LT) in spring, summer, and autumn to 8:00 LT in winter. Due to the increasing of boundary layer height or wind speed during the day. The BC concentration starts to decrease after the peak time until 15:00

LT. Then, as shown in Figure 5, BC concentration increased rapidly from 16:00 LT to the peak at 19:00 LT in autumn and winter, which increased slowly from the minimum and did not present significant peak in the evening in spring and summer. This indicates that the wood burning was most probably the important BC emission source during cold period. Another possible reason could be the boundary layer height decreased more rapidly to capture BC close to the earth surface in autumn and winter than that in spring and summer. The reduced human activities during the night hours would be the main reason for the observed lower BC concentration from the midnight until the morning rush hour in all seasons.

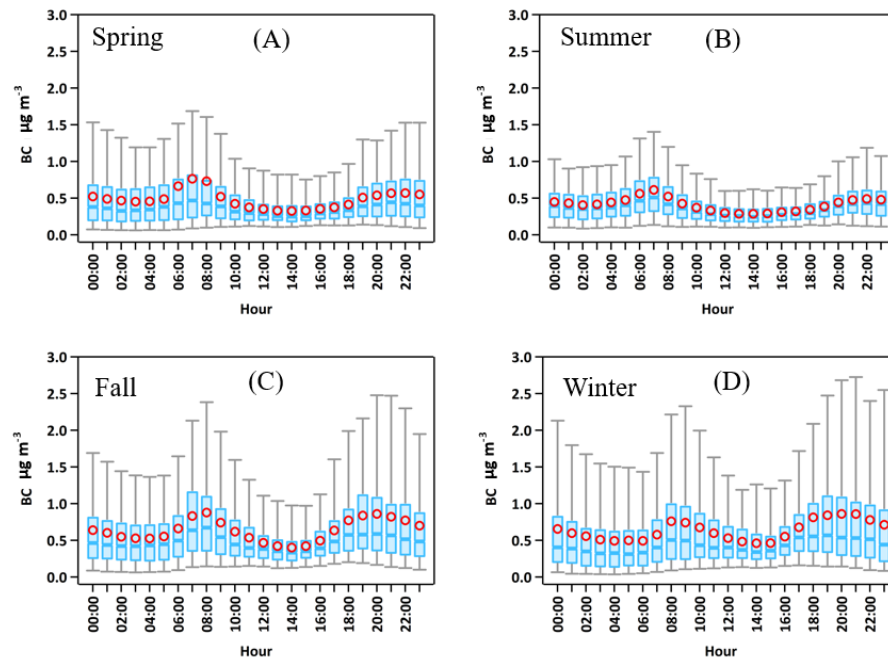


**Figure 3.** Average diurnal variations of BC during different seasons for the period 2017-2021.

### 3.3. Weekend effects

Overall, the BC concentration had a weekly cycle with slightly lower concentrations on weekends than during weekdays (Figure 6a,b). The daily median BC concentration ranged between 0.4-0.7  $\mu\text{g m}^{-3}$  and 0.3-0.5  $\mu\text{g m}^{-3}$  for weekdays and weekends, respectively. The diurnal variations of BC were different between the

weekdays and weekends, as shown in Figure 6. The weekdays presented two peaks pattern related to the morning and evening rush hours, but the weekends only showed slight increase in BC concentration from late afternoon. However, both weekdays and weekends had similar diurnal variation with the BC emission from fossil fuel which reveals that vehicle emission was the main BC source during the weekdays and less use of vehicle on weekends can significantly cut down the local BC concentration. Lower BC concentration on weekends compared to weekdays was also observed at traffic sites in other European cities like Bern and London (Reche et al., 2011) and Zurich (Zotter et al., 2017). Kutzner et al. (2018) reported negligible weekdays-weekends differences at urban background and industrial sites in Germany. As shown in Figure 6, a non-traffic source such as domestic heating could be another important BC source in the suburban site of our study.

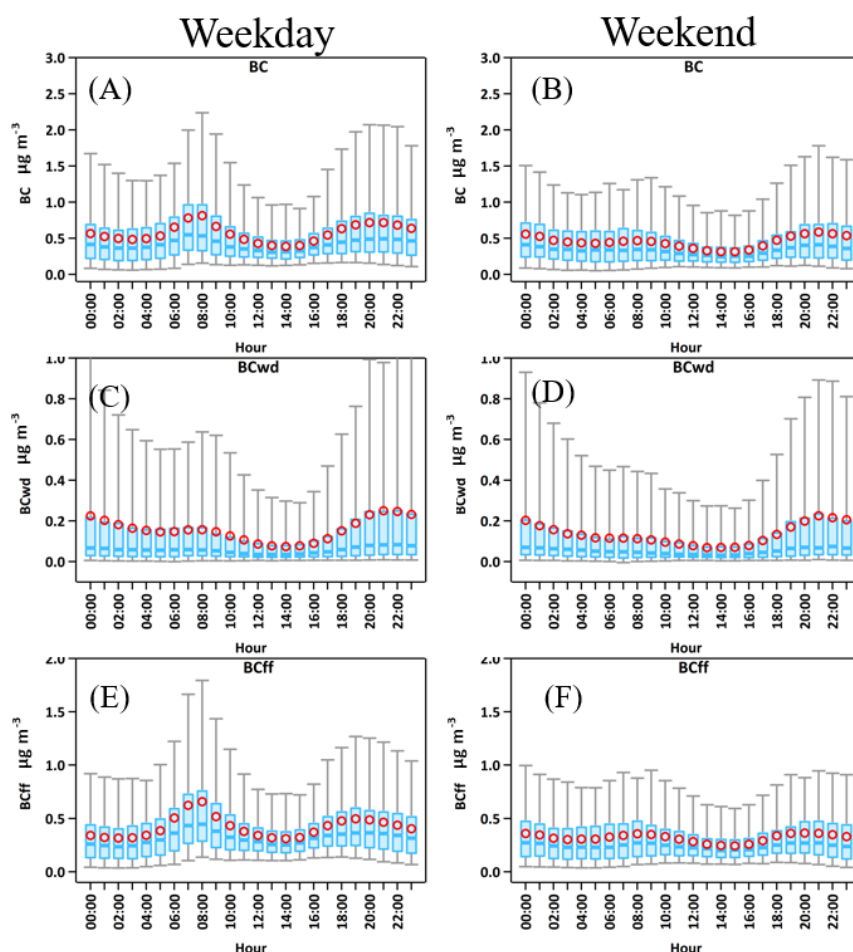


**Figure 4.** Average diurnal profiles of BC, BC<sub>wb</sub> and BC<sub>ff</sub> during weekends and weekdays.

### **3.4. COVID-19 Lockdown impact**

A number of studies have reported changes in the the observed concentration profiles of BC before, during and after the lockdown in some countries. For example, Jia et al. (2021) reported significant decline in the BC emission in eastern and northern China, respectively, 70% and 48%. Wei et al. (2022) observed a reduction of BC up to 0.06 mg/m<sup>2</sup> per day in northern India in April-May 2020 during COVID lockdown. We have compiled in Figure 7 the time series of BC concentrations before, during and after the three French lockdowns (first: 27 March–10 May 2020, second: 29 October–15 December 2020, third: 17 March–3 May 2021) measured in Orléans. The Figure shows that BC concentration increased in the first two days from 27 to 29 March 2020 after the French government announced the first lockdown. This may be attributed to the increased traffic activities for residents to buy the necessary living supplies. Then the BC concentration kept at a low level during the first lockdown and after the lockdown. The second lockdown in France was less strict than the first one with about 30% of the population allowed to go to work. The high BC concentrations observed during the second lockdown was attributed, at least partly, to emission from household wood burning since the temperature was low during this period. Relatively high BC concentrations were also observed during Christmas Holidays period from 25 December 2020 to 15 January 2021 which also may be due to household wood burning. During the third lockdown covering the period 17 March to 3 May 2021, low BC concentration was observed. The averaged BC, BC<sub>ff</sub> and BC<sub>wb</sub> concentration for these three lockdowns is presented in Figure 7. Interestingly, as shown in Figure 8, we found that BC emission from fossil fuel were at similar levels before, during and after these three lockdown periods, and the BC concentration changes was mainly due to the BC emission from wood burning. The reason could be that the location of the sampling site in this work was not impacted by heavy traffic and industries. This



284 observation is specific to the investigated site and the situation could be different in  
285 other areas such as Delhi (Goel et al., 2021) and Wuhan (Z. Wang et al., 2021). It is  
286 worth noting that in this study we just compared the observed BC concentrations but  
287 did not consider the meteorological impacts (e.g., from atmospheric dilution,  
288 boundary layer, etc.), which may add uncertainties.

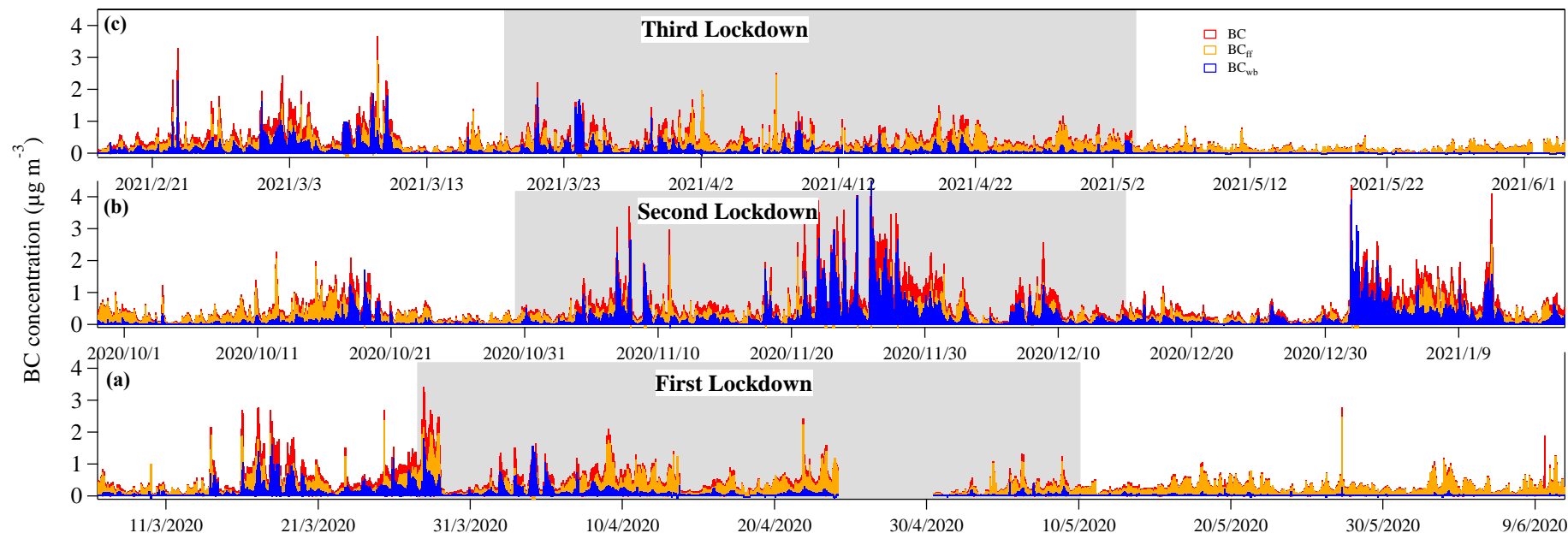


**Figure 7.** Time series of BC,  $BC_{ff}$  and  $BC_{wb}$  concentration for the three lockdowns in France, (a) First Lockdown: before lockdown (6 March–26 March 2020), during lockdown (27 March–10 May 2020) and after lockdown (11 May–10 June 2020); (b) Second lockdown: before lockdown (29 September–28 October 2020), during lockdown (29 October–15 December 2020) and after lockdown (16 December 2020–16 January 2021); (c) Third lockdown: before lockdown (17 February–16 March 2021), during lockdown (17 March–3 May 2021) and after lockdown (4 May–3 June 2021).

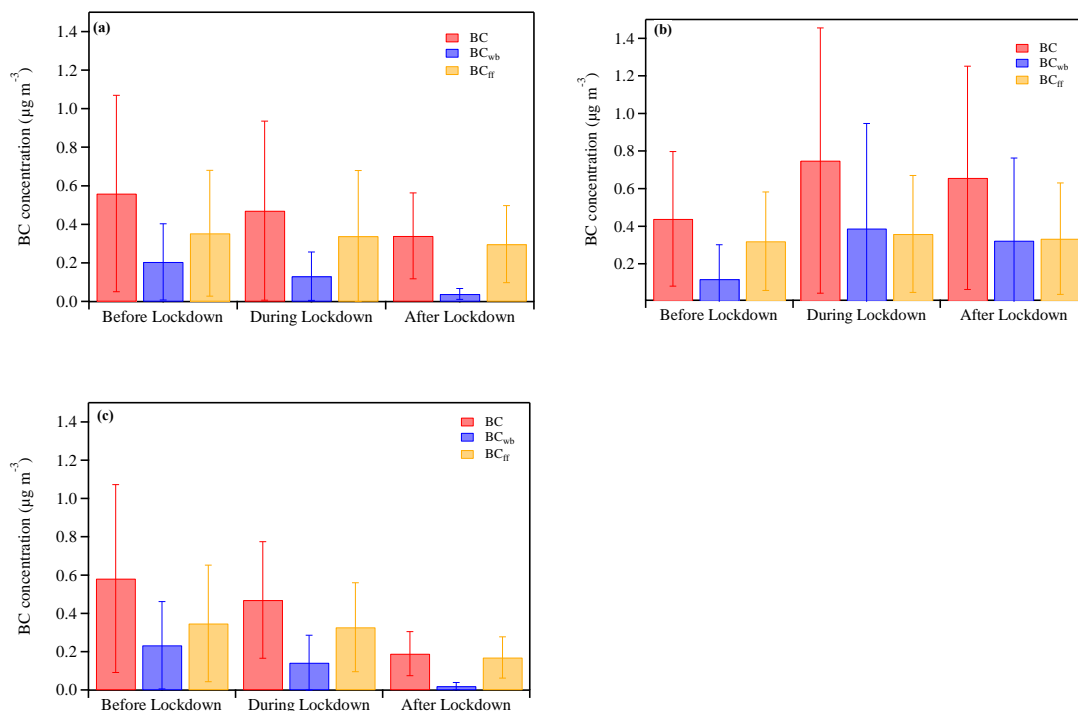


**Figure 8.** Column plots of average BC,  $\text{BC}_{\text{ff}}$  and  $\text{BC}_{\text{wb}}$  for the three lockdowns in France, (a) First Lockdown: before lockdown (6 March–26 March 2020), during lockdown (27 March–10 May 2020) and after lockdown (11 May–10 June 2020); (b) Second lockdown: before lockdown (29 September–28 October 2020), during lockdown (29 October–15 December 2020) and after lockdown (16 December 2020–16 January 2021); (c) Third lockdown: before lockdown (17 February–16 March 2021), during lockdown (17 March–3 May 2021) and after lockdown (4 May–3 June 2021).

### 3.5. Wood Burning vs. Fossil Fuel

To further discuss the BC sources in the suburban area of this work, a monthly average of  $\text{BC}_{\text{wb}}$  and  $\text{BC}_{\text{ff}}$  concentration and their contribution to total BC was depicted in Figure 9. The BC concentration peaked in late fall (November) and winter with maxima around  $0.86 \mu\text{g m}^{-3}$ . As shown in Figure 9A, BC from the combustion of fossil fuel ( $\text{BC}_{\text{ff}}$ ) showed a relatively flat seasonal cycle, roughly constant in the range  $0.29$  to  $0.50 \mu\text{g m}^{-3}$  throughout the year 2017 to 2021. To the contrast, BC from the

combustion of wood burning ( $BC_{wd}$ ) showed a more pronounced seasonal dependence, with negligible contribution ( $<0.05 \mu\text{g m}^{-3}$ ) from May to September and moderate contribution in other months ( $0.1\text{-}0.43 \mu\text{g m}^{-3}$ ). Consequently,  $BC_{ff}$  made dominate relative contribution to the observed BC throughout the whole year ( $>50\%$ , Figure 9B), particularly high contributions from May to September ( $>88\%$ , Figure 9B). This result is in good agreement with other reports indicating that in the majority of European cities, BC typically originates from traffic (Kutzner et al., 2018).

As discussed in the literatures (Becerril-Valle et al., 2017; Kumar et al., 2020; Mousavi et al., 2018) the monthly variation of  $BC_{ff}$  concentration in the year is mainly related to the weather conditions while that of  $BC_{bb}$  concentration is not only related to the weather conditions but also human activities, such as the straw burning in autumn, forest fire in summer and wood burning from domestic heating in winter. In this work (Figure 9), BC from the combustion of wood burning ( $BC_{wb}$ ) showed a more pronounced seasonal dependence, within negligible contribution to BC from May to September. The  $BC_{bb}$  concentrations tend to be higher in the cold seasons to contribute 22-50% to the total BC, which was likely related to the household heating, especially in the evening of winter as shown in Figure S2.

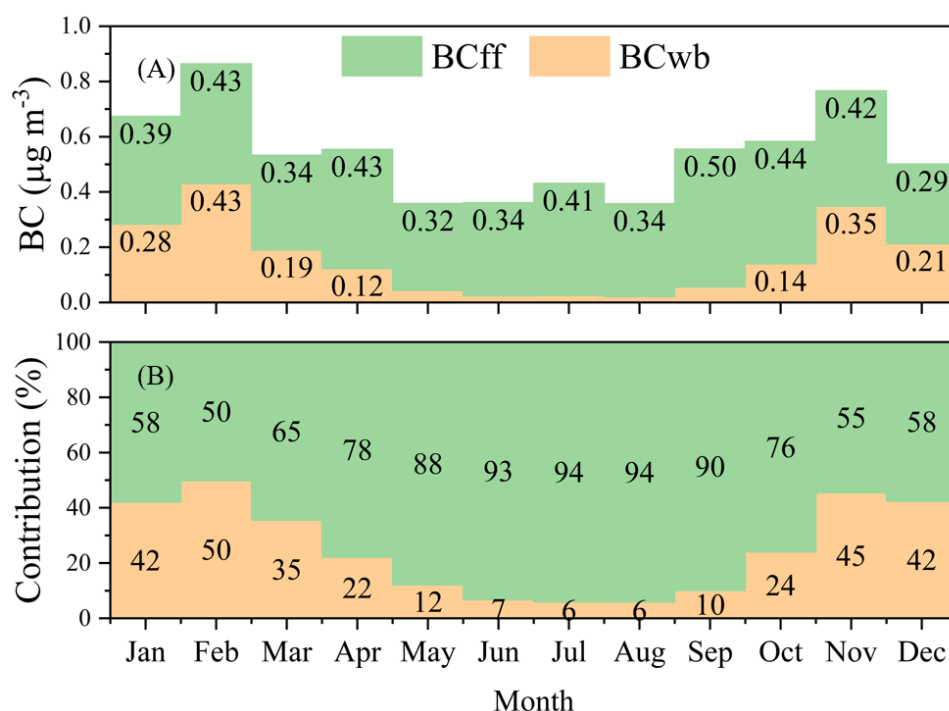


**Figure 9.** Monthly averages of  $BC_{wb}$  and  $BC_{ff}$  in Orléans city

#### 4. Conclusions and Implications

To investigate the variation and the long-term trend of BC, a nearly five-year BC measurement was conducted in a suburban area in central France. The BC annual mean concentration was calculated as  $0.75 \pm 0.65$ ,  $0.58 \pm 0.44$ ,  $0.54 \pm 0.64$ ,  $0.48 \pm 0.46$  and  $0.50 \pm 0.72 \mu g m^{-3}$ , respectively, for the year of 2017, 2018, 2019, 2020 and 2021, indicating a stability to a very slight decrease trend ( $-0.036 \mu g m^{-3} year^{-1}$ ) from 2017 to 2021. These BC concentrations were lower than that reported in some other cities. Strong BC seasonal variations were observed, with the highest BC concentrations occurred in winter, followed by autumn, spring and summer. A weekend effect was also observed in the measured area of this work, within generally slight high BC concentration during the workdays. Lower BC concentration was always observed during the weekends which was attributed to less traffic.

As for the COVID-19 measures impact, three successive lockdown periods have been followed in France, two in warm season (March to May) and one in cold season

(October to December). We found that the BC concentration decreased during the lockdown in the warm season, but unexpectedly increased during the lockdown in cold season, which was mainly caused by the variation of BC emission from biomass burning.

Fossil fuel contributed more than 90% of BC emission in the summer, much higher than that from wood burning. However, wood burning contributed equivalent (50%) to fossil fuel burning to the BC emission in the cold seasons, revealing the significant impact of winter heating from wood burning on regional air quality. Moreover, the above findings indicate that local anthropogenic emissions could strongly affect the BC concentration observed at the VOLTAIRE supersite as well as air quality in this region. Hence, the national level of strategies to improve air quality is always important, but also the local strategies toward reducing local emission such as domestic wood burning and fossil fuel combustion emissions.

#### **Credit authorship contribution statement**

EI Mehdi EI Baramoussi: Investigation, Formal analysis, Writing - original draft.  
Yangang Ren: Supervision, Investigation, Formal analysis, Writing - original draft.  
Chaoyang Xue: Investigation, Formal analysis, Writing - review & editing. Ibrahim Ouchen: Investigation. Véronique Daële: Investigation, Writing - review & editing.  
Patrick Mercier: Investigation. Christophe Chalumeau: Investigation. Frédéric LE Fur: Investigation. Patrice Colin: Investigation. Abderrazak Yahyaoui: Investigation.  
Oliver Favez: Investigation, Writing - review & editing. Abdelwahid Mellouki: Supervision, Project administration, Writing - review & editing.

#### **Declaration of competing interest**

The author declare that they have no known competing financial interests or personal relationships that could have appeared to influence the work reported in this paper.

## Acknowledgements

We thank le ministère en charge de l'environnement en France for the financement of mesures. C.X. thanks Cheng Wu (Jinan University) for providing the IGOR code for some data analysis shown in this study (Wu et al. ACP. 2018; <https://zenodo.org/record/832396>).

## Funding

This work was supported by the National Natural Science Foundation of China (21976106) and funding of youth scientist from Research Center for Eco-Environmental Sciences - Chinese Academy of Sciences (RCEES-CAS). This study was also supported by the VOLTAIRE project (ANR-10-LABX-100-01) funded by the ANR and the PIVOTS project provided by the Region Centre – Val de Loire (ARD 2020 program and CPER 2015 - 2020), and the Marie Skłodowska Curie Actions Programme (No. 690958) (MARSU).

## References

- AMAP, A.M. and A., 2015. AMAP Assessment 2015: Black carbon and ozone as Arctic climate forcers (Technical Report). Arctic Monitoring and Assessment Programme (AMAP).
- Anenberg, S.C., Talgo, K., Arunachalam, S., Dolwick, P., Jang, C., West, J.J., 2011. Impacts of global, regional, and sectoral black carbon emission reductions on surface air quality and human mortality. *Atmospheric Chem. Phys.* 11, 7253–7267. <https://doi.org/10.5194/acp-11-7253-2011>
- Becerril-Valle, M., Coz, E., Prévôt, A.S.H., Močnik, G., Pandis, S.N., Sánchez de la Campa, A.M., Alastuey, A., Díaz, E., Pérez, R.M., Artíñano, B., 2017. Characterization of atmospheric black carbon and co-pollutants in urban and rural areas of Spain. *Atmos. Environ.* 169, 36–53. <https://doi.org/10.1016/j.atmosenv.2017.09.014>
- Blanco-Donado, E.P., Schneider, I.L., Artaxo, P., Lozano-Osorio, J., Portz, L., Oliveira, M.L.S., 2022. Source identification and global implications of black carbon. *Geosci. Front.* 13, 101149. <https://doi.org/10.1016/j.gsf.2021.101149>
- Cui, S., Xian, J., Shen, F., Zhang, L., Deng, B., Zhang, Y., Ge, X., 2021. One-Year Real-Time Measurement of Black Carbon in the Rural Area of Qingdao,

410 Northeastern China: Seasonal Variations, Meteorological Effects, and the  
 411 COVID-19 Case Analysis. *Atmosphere* 12, 394.  
 412 <https://doi.org/10.3390/atmos12030394>  
 413 de Nazelle, A., Fruin, S., Westerdahl, D., Martinez, D., Ripoll, A., Kubesch, N.,  
 414 Nieuwenhuijsen, M., 2012. A travel mode comparison of commuters'  
 415 exposures to air pollutants in Barcelona. *Atmos. Environ.* 59, 151–159.  
 416 <https://doi.org/10.1016/j.atmosenv.2012.05.013>  
 417 Ding, A.J., Huang, X., Nie, W., Sun, J.N., Kerminen, V. - M., Petäjä, T., Su, H., Cheng,  
 418 Y.F., Yang, X. - Q., Wang, M.H., Chi, X.G., Wang, J.P., Virkkula, A., Guo,  
 419 W.D., Yuan, J., Wang, S.Y., Zhang, R.J., Wu, Y.F., Song, Y., Zhu, T.,  
 420 Zilitinkevich, S., Kulmala, M., Fu, C.B., 2016. Enhanced haze pollution by  
 421 black carbon in megacities in China. *Geophys. Res. Lett.* 43, 2873–2879.  
 422 <https://doi.org/10.1002/2016GL067745>  
 423 Franco, J.F., Segura, J.F., Mura, I., 2016. Air Pollution alongside Bike-Paths in  
 424 Bogotá-Colombia. *Front. Environ. Sci.* 4.  
 425 <https://doi.org/10.3389/fenvs.2016.00077>  
 426 Fuller, G.W., Tremper, A.H., Baker, T.D., Yttri, K.E., Butterfield, D., 2014.  
 427 Contribution of wood burning to PM<sub>10</sub> in London. *Atmos. Environ.* 87, 87–94.  
 428 <https://doi.org/10.1016/j.atmosenv.2013.12.037>  
 429 Garrido, A., Jiménez-Guerrero, P., Ratola, N., 2014. Levels, trends and health concerns  
 430 of atmospheric PAHs in Europe. *Atmos. Environ.* 99, 474–484.  
 431 <https://doi.org/10.1016/j.atmosenv.2014.10.011>  
 432 Genberg, J., Denier van der Gon, H.A.C., Simpson, D., Swietlicki, E., Areskou, H.,  
 433 Beddows, D., Ceburnis, D., Fiebig, M., Hansson, H.C., Harrison, R.M.,  
 434 Jennings, S.G., Saarikoski, S., Spindler, G., Visschedijk, A.J.H., Wiedensohler,  
 435 A., Yttri, K.E., Bergström, R., 2013. Light-absorbing carbon in Europe –  
 436 measurement and modelling, with a focus on residential wood combustion  
 437 emissions. *Atmospheric Chem. Phys.* 13, 8719–8738.  
 438 <https://doi.org/10.5194/acp-13-8719-2013>  
 439 Goel, V., Hazarika, N., Kumar, M., Singh, V., Thamban, N.M., Tripathi, S.N., 2021.  
 440 Variations in Black Carbon concentration and sources during COVID-19  
 441 lockdown in Delhi. *Chemosphere* 270, 129435.  
 442 <https://doi.org/10.1016/j.chemosphere.2020.129435>  
 443 Gong, T., Sun, Z., Zhang, X., Zhang, Y., Wang, S., Han, L., Zhao, D., Ding, D., Zheng,  
 444 C., 2019. Associations of black carbon and PM<sub>2.5</sub> with daily cardiovascular  
 445 mortality in Beijing, China. *Atmos. Environ.* 214, 116876.  
 446 <https://doi.org/10.1016/j.atmosenv.2019.116876>  
 447 Hankey, S., Marshall, J.D., 2015. Land Use Regression Models of On-Road Particulate  
 448 Air Pollution (Particle Number, Black Carbon, PM<sub>2.5</sub>, Particle Size) Using  
 449 Mobile Monitoring. *Environ. Sci. Technol.* 49, 9194–9202.  
 450 <https://doi.org/10.1021/acs.est.5b01209>



- Jarjour, S., Jerrett, M., Westerdahl, D., de Nazelle, A., Hanning, C., Daly, L., Lipsitt, J., Balmes, J., 2013. Cyclist route choice, traffic-related air pollution, and lung function: a scripted exposure study. *Environ. Health* 12, 14. <https://doi.org/10.1186/1476-069X-12-14>
- Jia, M., Evangeliou, N., Eckhardt, S., Huang, X., Gao, J., Ding, A., Stohl, A., 2021. Black Carbon Emission Reduction Due to COVID- 19 Lockdown in China. *Geophys. Res. Lett.* 48. <https://doi.org/10.1029/2021GL093243>
- Krecl, P., Johansson, C., Ström, J., Lövenheim, B., Gallet, J.-C., 2014. A feasibility study of mapping light-absorbing carbon using a taxi fleet as a mobile platform. *Tellus B Chem. Phys. Meteorol.* 66, 23533. <https://doi.org/10.3402/tellusb.v66.23533>
- Krecl, P., Targino, A.C., Landi, T.P., Ketznel, M., 2018. Determination of black carbon, PM<sub>2.5</sub>, particle number and NO<sub>x</sub> emission factors from roadside measurements and their implications for emission inventory development. *Atmos. Environ.* 186, 229–240. <https://doi.org/10.1016/j.atmosenv.2018.05.042>
- Kumar, R.R., Soni, V.K., Jain, M.K., 2020. Evaluation of spatial and temporal heterogeneity of black carbon aerosol mass concentration over India using three year measurements from IMD BC observation network. *Sci. Total Environ.* 723, 138060. <https://doi.org/10.1016/j.scitotenv.2020.138060>
- Kutzner, R.D., von Schneidmesser, E., Kuik, F., Quedenau, J., Weatherhead, E.C., Schmale, J., 2018. Long-term monitoring of black carbon across Germany. *Atmos. Environ.* 185, 41–52. <https://doi.org/10.1016/j.atmosenv.2018.04.039>
- Lei, X., Bian, J., Xiu, G., Hu, X., Gu, X., Bian, Q., 2017. The mobile monitoring of black carbon and its association with roadside data in the Chinese megacity of Shanghai. *Environ. Sci. Pollut. Res.* 24, 7482–7489. <https://doi.org/10.1007/s11356-017-8454-2>
- Li, J., Fu, Q., Huo, J., Wang, D., Yang, W., Bian, Q., Duan, Y., Zhang, Y., Pan, J., Lin, Y., Huang, K., Bai, Z., Wang, S.-H., Fu, J.S., Louie, P.K.K., 2015. Tethered balloon-based black carbon profiles within the lower troposphere of Shanghai in the 2013 East China smog. *Atmos. Environ.* 123, 327–338. <https://doi.org/10.1016/j.atmosenv.2015.08.096>
- Li, Y., Henze, D.K., Jack, D., Henderson, B.H., Kinney, P.L., 2016. Assessing public health burden associated with exposure to ambient black carbon in the United States. *Sci. Total Environ.* 539, 515–525. <https://doi.org/10.1016/j.scitotenv.2015.08.129>
- Liu, B., He, M.M., Wu, C., Li, J., Li, Y., Lau, N.T., Yu, J.Z., Lau, A.K.H., Fung, J.C.H., Hoi, K.I., Mok, K.M., Chan, C.K., Li, Y.J., 2019. Potential exposure to fine particulate matter (PM<sub>2.5</sub>) and black carbon on jogging trails in Macau. *Atmos. Environ.* 198, 23–33. <https://doi.org/10.1016/j.atmosenv.2018.10.024>
- Liu, M., Peng, X., Meng, Z., Zhou, T., Long, L., She, Q., 2019. Spatial characteristics and determinants of in-traffic black carbon in Shanghai, China: Combination of

mobile monitoring and land use regression model. *Sci. Total Environ.* 658, 51–61. <https://doi.org/10.1016/j.scitotenv.2018.12.135>

Mousavi, A., Sowlat, M.H., Hasheminassab, S., Polidori, A., Sioutas, C., 2018. Spatio-temporal trends and source apportionment of fossil fuel and biomass burning black carbon (BC) in the Los Angeles Basin. *Sci. Total Environ.* 640–641, 1231–1240. <https://doi.org/10.1016/j.scitotenv.2018.06.022>

Okokon, E.O., Yli-Tuomi, T., Turunen, A.W., Taimisto, P., Pennanen, A., Vouitsis, I., Samaras, Z., Voogt, M., Keuken, M., Lanki, T., 2017. Particulates and noise exposure during bicycle, bus and car commuting: A study in three European cities. *Environ. Res.* 154, 181–189. <https://doi.org/10.1016/j.envres.2016.12.012>

Pörtner, H.-O., Roberts, D.C., Tignor, M.M.B., Poloczanska, E.S., Mintenbeck, K., Alegría, A., Craig, M., Langsdorf, S., Löschke, S., Möller, V., Okem, A., Rama, B. (Eds.), 2022. *Climate Change 2022: Impacts, Adaptation and Vulnerability. Contribution of Working Group II to the Sixth Assessment Report of the Intergovernmental Panel on Climate Change.*

Reche, C., Querol, X., Alastuey, A., Viana, M., Pey, J., Moreno, T., Rodríguez, S., González, Y., Fernández-Camacho, R., de la Rosa, J., Dall’Osto, M., Prévôt, A.S.H., Hueglin, C., Harrison, R.M., Quincey, P., 2011. New considerations for PM, Black Carbon and particle number concentration for air quality monitoring across different European cities. *Atmospheric Chem. Phys.* 11, 6207–6227. <https://doi.org/10.5194/acp-11-6207-2011>

Sand, M., Berntsen, T.K., von Salzen, K., Flanner, M.G., Langner, J., Victor, D.G., 2016. Response of Arctic temperature to changes in emissions of short-lived climate forcers. *Nat. Clim. Change* 6, 286–289. <https://doi.org/10.1038/nclimate2880>

Sandradewi, J., Prévôt, A.S.H., Szidat, S., Perron, N., Alfarra, M.R., Lanz, V.A., Weingartner, E., Baltensperger, U., 2008. Using Aerosol Light Absorption Measurements for the Quantitative Determination of Wood Burning and Traffic Emission Contributions to Particulate Matter. *Environ. Sci. Technol.* 42, 3316–3323. <https://doi.org/10.1021/es702253m>

Silva, R.A., West, J.J., Zhang, Y., Anenberg, S.C., Lamarque, J.-F., Shindell, D.T., Collins, W.J., Dalsoren, S., Faluvegi, G., Folberth, G., Horowitz, L.W., Nagashima, T., Naik, V., Rumbold, S., Skeie, R., Sudo, K., Takemura, T., Bergmann, D., Cameron-Smith, P., Cionni, I., Doherty, R.M., Eyring, V., Josse, B., MacKenzie, I.A., Plummer, D., Righi, M., Stevenson, D.S., Strode, S., Szopa, S., Zeng, G., 2013. Global premature mortality due to anthropogenic outdoor air pollution and the contribution of past climate change. *Environ. Res. Lett.* 8, 034005. <https://doi.org/10.1088/1748-9326/8/3/034005>

531 Singh, V., Ravindra, K., Sahu, L., Sokhi, R., 2018. Trends of atmospheric black carbon  
532 concentration over the United Kingdom. *Atmos. Environ.* 178, 148–157.  
533 <https://doi.org/10.1016/j.atmosenv.2018.01.030>

534 Sun, J., Birmili, W., Hermann, M., Tuch, T., Weinhold, K., Merkel, M., Rasch, F.,  
535 Müller, T., Schladitz, A., Bastian, S., Löschau, G., Cyrys, J., Gu, J., Flentje, H.,  
536 Briel, B., Asbach, C., Kaminski, H., Ries, L., Sohmer, R., Gerwig, H., Wirtz, K.,  
537 Meinhardt, F., Schwerin, A., Bath, O., Ma, N., Wiedensohler, A., 2020.  
538 Decreasing trends of particle number and black carbon mass concentrations at  
539 16 observational sites in Germany from 2009 to 2018. *Atmospheric Chem. Phys.*  
540 20, 7049–7068. <https://doi.org/10.5194/acp-20-7049-2020>

541 Targino, A.C., Gibson, M.D., Krecl, P., Rodrigues, M.V.C., dos Santos, M.M., de  
542 Paula Corrêa, M., 2016. Hotspots of black carbon and PM<sub>2.5</sub> in an urban area  
543 and relationships to traffic characteristics. *Environ. Pollut.* 218, 475–486.  
544 <https://doi.org/10.1016/j.envpol.2016.07.027>

545 Wang, Y., Li, X., Shi, Z., Huang, L., Li, J., Zhang, H., Ying, Q., Wang, M., Ding, D.,  
546 Zhang, X., Hu, J., 2021. Premature Mortality Associated with Exposure to  
547 Outdoor Black Carbon and Its Source Contributions in China. *Resour. Conserv.*  
548 *Recycl.* 170, 105620. <https://doi.org/10.1016/j.resconrec.2021.105620>

549 Wang, Z., Ehn, M., Rissanen, M.P., Garmash, O., Quéléver, L., Xing, L.,  
550 Monge-Palacios, M., Rantala, P., Donahue, N.M., Berndt, T., Sarathy, S.M.,  
551 2021. Efficient alkane oxidation under combustion engine and atmospheric  
552 conditions. *Commun. Chem.* 4, 18.  
553 <https://doi.org/10.1038/s42004-020-00445-3>

554 Wei, L., Lu, Z., Wang, Y., Liu, X., Wang, W., Wu, C., Zhao, X., Rahimi, S., Xia, W.,  
555 Jiang, Y., 2022. Black carbon-climate interactions regulate dust burdens over  
556 India revealed during COVID-19. *Nat. Commun.* 13, 1839.  
557 <https://doi.org/10.1038/s41467-022-29468-1>

558 WHO, 2012. Sixty-fifth World Health Assembly, Resolutions and Decisions. World  
559 Health Organ. WHO.

560 Williams, R.D., Knibbs, L.D., 2016. Daily personal exposure to black carbon: A pilot  
561 study. *Atmos. Environ.* 132, 296–299.  
562 <https://doi.org/10.1016/j.atmosenv.2016.03.023>

563 WMO, 2016. The global climate in 2011-2015, World Meteorological Organization.  
564 World Meteorological Organization, Geneva.

565 Zhang, F., Wang, Yuan, Peng, J., Chen, L., Sun, Y., Duan, L., Ge, X., Li, Y., Zhao, J.,  
566 Liu, C., Zhang, X., Zhang, G., Pan, Y., Wang, Yuesi, Zhang, A.L., Ji, Y., Wang,  
567 G., Hu, M., Molina, M.J., Zhang, R., 2020. An unexpected catalyst dominates  
568 formation and radiative forcing of regional haze. *Proc. Natl. Acad. Sci.* 117,  
569 3960–3966. <https://doi.org/10.1073/pnas.1919343117>

570 Zotter, P., Herich, H., Gysel, M., El-Haddad, I., Zhang, Y., Močnik, G., Hüglin, C.,  
571 Baltensperger, U., Szidat, S., Prévôt, A.S.H., 2017. Evaluation of the absorption

572 Ångström exponents for traffic and wood burning in the Aethalometer-based  
573 source apportionment using radiocarbon measurements of ambient aerosol.  
574 Atmospheric Chem. Phys. 17, 4229–4249.  
575 <https://doi.org/10.5194/acp-17-4229-2017>  
576